Special Issue – Imaging Cell Biology

Imaging endocytic clathrin structures in living cells

Tom Kirchhausen

Harvard Medical School/ Immune Disease Institute, W. Alpert Building Room 128, 200 Longwood Ave, Boston, MA 02115, USA

Our understanding of the clathrin-dependent endocytic pathway owes much to new visualization techniques. Budding coated pits and clathrin-coated structures are transient molecular machines with distinctive morphological characteristics, and fluorescently labeled versions of a variety of marker proteins have given us a tantalizing glimpse of the dynamics of the system in living cells. Recent live-cell imaging studies have revealed unexpected modes of coat assembly, with distinct kinetics, distinct recruitment of associated proteins, distinct requirements for the participation of actin and its accessory proteins, and apparently distinct mechanisms of membrane deformation. A crucial issue is to connect the events detected by light microscopy with the structures and properties of the molecular constituents. Here, I outline descriptions of coat assembly in different circumstances that are consistent with what is known from X-ray crystallography and electron microscopy.

The need to analyze endocytosis in live cells

Cells require ordered movement of proteins and lipids from one membrane-bound compartment to another. The most common mechanism for such transport is the formation and budding of a vesicle from the membrane of a donor compartment and fusion of the vesicle with the membrane of an acceptor compartment. This process maintains the organization, function and heterogeneity of the donor and acceptor membranes. The molecular machinery scaffolded by clathrin is a particularly well-defined and physiologically important example of vesicle formation. Assembly of a clathrin coat at a donor membrane deforms and invaginates a membrane patch, which, after pinching and scission, becomes a carrier of membrane traffic. Clathrin-coated vesicles are the most prominent form of traffic from the plasma membrane to endosomes (endocytosis), a pathway by which ligands, such as hormones and other signaling molecules, transferrin, immunoglobulins, low-density lipoproteins (LDLs), viruses and their receptors, enter cells. Clathrin coats are also important for traffic between endosomes and the *trans*-Golgi network (TGN) [1–9].

The 'life cycle' of a clathrin-coated vesicle, from coat assembly and cargo loading to coat disassembly and cargo delivery, involves a large number of structural and regulatory proteins and lipids. These components are often present in small amounts. They participate in a series of rapid, regulated events (Figure 1) (Box 1), and their study, therefore, poses particular challenges, both for the strategies required to trap a defined state of a dynamic assembly and the technologies needed to follow its normal cycle in cells.

Cellular, biochemical and high-resolution structural approaches have defined the molecular properties of clathrin and many of its associated proteins [1,10–17]. Biochemical and structural approaches, however powerful, can only provide snapshots or ensemble-averaged information about the properties of objects within a heterogeneous population. They are not sufficient to resolve important steps in vesicle formation and uncoating. Advanced imaging methods can now achieve high temporal resolution in the context of a living cell [18,19], allowing one to localize components during a given step to determine the order in which components are incorporated or released and analyze the way the composition of an assembling vesicle affects its behavior [20–34]. So far, most studies have focused on endocytosis. This is a particularly favorable membrane traffic pathway for such studies because labeled cargo can be prepared and followed, thereby identifying functional uptake, and because events at the cell surface are particularly accessible to live-cell imaging methods.

This review focuses on the interpretation of results from live-cell imaging, rather than on the data obtained using fixed samples that, in principle, could provide improved spatial resolution [35,36] but at the cost of losing the temporal component. Gathering data over time is essential for analyzing highly dynamic systems such as those that direct membrane traffic. A central issue in developing models to describe the dynamics of clathrin coat formation is how to relate the data from live-cell imaging to the static morphological information obtained from cells by electron microscopy and the high-resolution structures obtained from X-ray crystallography and advanced electron cryo-microscopy (cryoEM). Correlation between distinguishable classes of clathrin-based endocytic events detected by fluorescence microscopy with their corresponding morphologies as seen by electron microscopy resolves a number of previous conflicts and misconceptions. These distinctions make our picture of clathrin dynamics consistent with the molecular structures defined by high-resolution methods.

Live-cell imaging of clathrin-coated structures

The advent of GFP combined with time-lapse wide-field epifluorescence microscopy (Box 2) provided the first
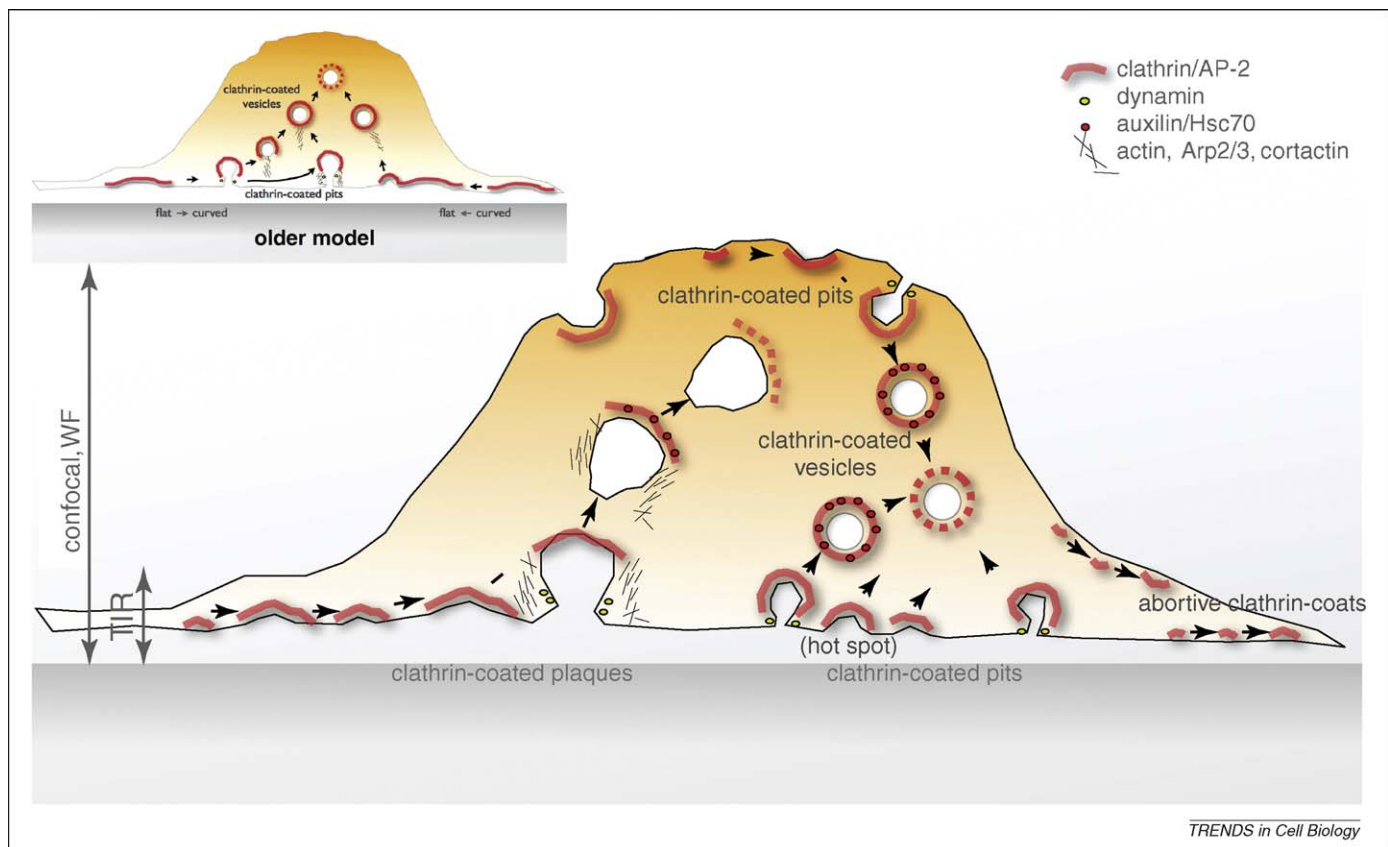

Figure 1. Formation of endocytic clathrin-coated structures on the plasma membrane of mammalian cells. The continuous line represents the plasma membrane of a cell grown in culture; the thick, pink stripe represents the clathrin coat (clathrin plus the AP-2 adaptor); yellow dots represent dynamin; red dots, the uncoating ATP Hsc70 and its cofactor auxilin; short thin lines, short-branched actin polymers plus the Arp2/3 complex, cortactin and N-Wasp. The stippled thick pink stripe represents the ATP-dependent dissolution of the clathrin coat mediated by Hsc70 and auxilin. TIR, wide-field and spinning disc confocal microscopy were all used to obtain live-cell imaging data; the vertical arrows indicate the *z*-positions accessible to each imaging method. Stable and transient expression of recombinant, fluorescently-tagged constructs were used to follow the dynamic behavior of plasma membrane structures containing different combinations of clathrin, AP-2, auxilin, Arp2/3 complex, cortactin and dynamin. Canonical clathrin-coated pits form at both the free and attached cell surfaces; clathrin-coated plaques form only at the attached surface. Coated pit formation proceeds by the sequential addition of clathrin triskelions to an initial nucleus, generating a sharply curved coat; adaptor-mediated interactions with membrane-bound proteins (and lipids) deform the underlying membrane; dynamin mediates scission when the deformation has created a suitably narrow neck; auxilin, which arrives immediately following scission, recruits the uncoating ATPase Hsc70. The relatively long-lasting clathrin-coated plaques probably initiate in a fashion similar to coated pits, but the subsequent addition of clathrin triskelions maintains a relatively flat structure with mainly hexagonal facets. The number of clathrin triskelions and AP-2 complexes associated with a clathrin-coated plaque can fluctuate during its lifetime. Coated plaques drive membrane invagination when the entire coat moves rapidly inwards, a step that requires the formation of short-branched actin filaments; by contrast, actin polymerization does not generally accompany the assembly or budding of coated pits. Abortive clathrin coats are incomplete, short-lived structures that fail to associate with cargo. Inset: diagram illustrating an older model, in which a flat coated plaque deforms into a sharply invaginated coated pit. Such a transformation is structurally implausible, as discussed in the text and illustrated by the exercise in Figure 5.

glimpse of assembling clathrin-coated structures in cells expressing the clathrin light chain LCa fused to GFP and demonstrated their transient character [29]. Although the time series were obtained from an optical plane close to the cell surface attached to the coverslip, thereby providing images of endocytic clathrin structures assembling at the plasma membrane, fluorescent objects located further inside the cell, probably clathrin coats on endosomal membranes, also contributed significantly to the data sets, leading to ambiguities in the interpretation. This limitation was soon overcome by the use of total internal reflection fluorescence (TIRF) microscopy, a powerful approach that is naturally suited to observing fluorescent events at the cell surface in contact with the glass coverslip [25].

Time-lapse TIRF of cells expressing the clathrin light chain fused to dsRED confirmed the dynamic character of endocytic structures and revealed their inward movement before the dissolution of the clathrin coat [25,26]. To obtain temporal information regarding the time of membrane scission from the donor plasma membrane of the budding

clathrin-coated membrane, a visual method was used to detect the exposure or protection from the incubation medium of the ectodomain of the transferrin (Tf) receptor [26]. A chimeric protein was constructed from the Tf receptor, fused in its ectodomain with pHluorin, a GFP-based fluorescent pH sensor. With this probe, the fluorescence of pHluorin-tagged Tf receptors located at the cell surface is sensitive to the pH of the incubating medium, whereas the fluorescence of those present in completely sealed intracellular vesicles is not. By cyclically alternating the pH of the incubating medium between pH 7.4 and 5.5, it was possible to detect a sudden loss in pH-dependence in the fluorescence signal of a subset of chimeric Tf receptor clusters associated with clathrin coats. The combined used of TIR and wide-field fluorescence imaging revealed that a pH-independent spot of the Tf receptor chimera appeared just as its associated fluorescent clathrin patch underwent abrupt inward movement. These observations provided the first direct link between the invagination step of a clathrin-coated structure and membrane scission [26].

Box 1. Clathrin and its partners

Abortive clathrin coat: a short-lived clathrin assembly that dissociates without internalizing membrane.

Actin, cortactin, Arp2/3 complex, N-Wasp: the Arp2/3 complex nucleates actin polymerization into short-branched filaments. Proteins that regulate this process include cortactin, N-Wasp and Cdc42.

AP-2: the main endocytic clathrin adaptor. It comprises four subunits: the large α- and β-adaptins; the medium μ2 adaptin; and the small σ2-adaptin. AP-2 has a key role in coat assembly under physiological conditions, a process mediated by its interactions with clathrin. AP-2 selectively binds to the phosphoinositide phosphatidylinositol (4,5)-bisphosphate [PtdIns(4,5)P_2] and to short peptide motifs present in the cytosolic tail of membrane-bound cargo receptors. It also binds to a number of other proteins, some of which can also interact with cargo receptors. The function AP-2 is, therefore, essential for the specific entrapment and sorting of cargo into clathrin-coated structures.

Auxilin, Hsc70: auxilin is a J-domain-containing protein that binds to the chaperone Hsc70, clathrin, AP-2 and phosphoinositides. The recruitment of auxilin to clathrin coats occurs after membrane scission; it in turn recruits Hsc70 to the clathrin coat, so that an ATP-dependent uncoating reaction can ensue.

Clathrin: a trimer of three ~190 kDa heavy chains, each with an associated 23–26 kDa light chain. The heavy chain has a very elongated structure, approximately 450 Å in contour length, with 42 α-helical zig-zags connecting a globular N terminal domain with a C terminal trimer hub. The light chains bind near the hub. The overall shape resembles the three-legged 'triskelion' in various traditional emblems. A clathrin triskelion is the assembly unit of a vesicular coat. It forms a curved polygonal lattice, with open hexagonal and pentagonal facets and the hub of a triskelion centered at each vertex. Each leg of a clathrin triskelion extends around three lattice edges.

Clathrin-coated pit: a sharp membrane invagination produced by the assembly of a clathrin coat. The radius of membrane curvature can range from 200 Å to more than 800 Å, and the radius of the polymerized coat from approximately 350 Å to more than 1000 Å. The coat ultimately closes in on itself, driving the formation of a narrow membrane neck.

Clathrin-coated plaque: an extended, relatively flat clathrin array, often found at an adherent surface of a cell in culture.

Dynamin: a large GTPase recruited to clathrin coats when the lattice is nearly complete; its function is essential for membrane scission.

Dynasore: the term originates from combining 'dyna' (dynamin) and 'sore' (pain). A cell-permeable small molecule that rapidly (and reversibly) inhibits dynamin function. It is widely used to interfere acutely with the cellular function of dynamin.

Hot spot: a more-or-less diffraction-limited region on a cell surface from which repeated clathrin-coated vesicles are seen to emanate. The hot-spot area can also contain a more stationary, long-lived clathrin assembly.

Box 2. A close-up view of microscopy terms

Diffraction limit: the resolution of an optical system, as defined by the classical Rayleigh criterion. In practical terms, the diffraction limit for fluorescence microscopy is ~250 nm in the *xy*-plane and ~500–800 nm in the *z* plane.

DiNa: 'differential evanescence nanometry', a method based on TIR and wide-field illumination to determine the axial separation of the centroids of two different fluorophore distributions with a precision of ~10 nm. This method was used in real time for the differential localization of AP-2 and epsin with respect to clathrin during the formation of clathrin-coated pits and plaques [22].

Laser-scanning confocal microscopy: in a confocal microscope, the illuminating beam converges on the focal plane; fluorescent radiation from the point of illumination will then converge on the conjugate point in the image plane, and a pinhole can be used to eliminate fluorescence from out-of-focus planes. Scanning the beam on an *xy*-raster over a succession of suitably spaced focal planes allows one to build up a 3D image. Data are collected with a photomultiplier detector and the image reconstructed computationally.

Spinning disc confocal microscopy: by arranging a set of microlenses and pinholes in an appropriate array on a rapidly rotating wheel, a confocal microscope can be constructed that repeatedly scans many points in parallel, thereby greatly increasing the rate of data acquisition, while decreasing phototoxicity. An image for each focal plane is collected on a standard CCD camera. With currently available laser illumination, it is possible to acquire single frame images in a few milliseconds. This makes spinning disc confocal microscopy a relatively straightforward way to achieve high temporal and spatial resolution for dynamic structures.

Total internal reflection fluorescence (TIRF) microscopy: total internal reflection (TIR) occurs when a beam of light is incident at a suitably small angle from a medium of higher refractive index onto an interface with a medium of lower refractive index. In particular, light is totally reflected when incident from a glass coverslip (n~1.5) onto the aqueous medium of a cell in culture (n~1.35). There is nonetheless an 'evanescent wave' produced in the lower refractive index medium, with an intensity that falls off exponentially as the distance from the interface grows. Thus, if the excitation illumination in a fluorescence microscope is so directed that it is totally reflected from the interface between the coverslip and adherent cell, fluorophores located within 100–200 nm of the coverslip are strongly excited, but those further away are not. Thus, the images of the layer at or near the cell surface contain little or no interference from fluorescent molecules elsewhere in the cytosol.

Wide-field illumination fluorescence microscopy: visualization using excitation illumination propagating parallel to the *z*-axis. The intensity of fluorescent molecules is directly proportional to their number within the illuminated volume. Images generated in this way have significant contributions from objects located above or below the focal plane. Spatial deconvolution is required for accurate representation of the image.

Other studies based on TIRF or spinning disc confocal microscopy followed the temporal recruitment of dynamin, the large GTPase required for the scission of the membrane neck connecting invaginating clathrin-coated pits from the plasma membrane [25,30,37,38]. The live-cell imaging data obtained alone or in combination with dynasore, a cell-permeable chemical compound that acutely inhibits the function of dynamin, revealed both the expected burst of dynamin recruitment upon completion of coat assembly and unexpected recruitment of a small amount of dynamin during the clathrin coat assembly process [37]. Although it is clear that the function of dynamin recruitment at the end of coat assembly is directly linked to the scission of the neck between the plasma membrane and the underlying coated membrane,

the role of dynamin recruited before membrane scission remains to be determined.

Motivated by the observation that, in yeast cells, endocytosis requires both clathrin- and actin- based components [39,40], several studies used TIRF, mainly in HeLa cells and fibroblasts, to explore the temporal recruitment of actin and a subset of regulators of short-branch actin assembly, including Arp2/3, cortactin and N-Wasp [26,27,41–43]. In general, most of the clathrin-containing fluorescent objects tracked in these experiments were relatively long-lived, with life spans of two minutes or more, and they seldom showed a steady increase in fluorescence during the lifetime of the clathrin-coated structure; the remaining clathrin objects were either shorter-lived, with life spans of approximately one minute, or appeared as small (diffraction

limited) structures detaching from larger ones. Many of these structures recruited actin, Arp2/3 complex or cortactin at or near the time of membrane scission, but others did not [21,25,26]. These studies led to the conclusion that, in mammalian cells as in yeast, actin is a key participant in clathrin-based endocytosis and its assembly is required to drive the inward movement of the budding clathrin-coated vesicle [21,26].

The observations summarized above were at odds with the variable dependence of clathrin traffic on actin polymerization, as defined by pharmacological criteria (sensitivity to actin depolymerizers, etc.) [44]. In some cases, for example the formation of clathrin-coated vesicles in presynaptic terminals of giant synapses from lampreys [45,46], or in the apical surface of polarized epithelial cells [47,48], and in the internalization of vesicular stomatitis virus (VSV) by clathrin-coated structures [49], actin polymerization is indeed linked to membrane deformation in clathrin-coated pits. However, in many other cases – for example endocytosis in the presynapse of rat hippocampal neurons [50] or transferrin uptake by coated pits of non-polarized BSC1 fibroblastic cells in culture [34,51] – actin polymerization is clearly not essential. We can now distinguish between at least two modes of clathrin coat formation at the plasma membrane, with different mechanisms for coat internalization (Figure 1). At one end of the spectrum, the actin cytoskeleton is not required for the normal formation and budding of the rapidly growing pits, whereas at the other it is essential for the formation, inward movement and dissolution of longer-lived clathrin structures. That is, clathrin is a scaffold for at least two kinds of membrane-associated processes. This distinction allows the resolution of apparent contradictions between the high-resolution structural data and some models put forward to explain how the invagination of clathrin-coated structures might occur (Figure 1, inset).

Distinct forms of endocytic clathrin-coated structures

Spinning disc confocal microscopy – another sensitive and rapid imaging approach – has been used to observe the assembly and disassembly dynamics of fluorescent clathrin structures as they form at the free plasma membrane at the free (top) and attached (bottom) surfaces of cells in culture (Figure 2a). These studies began with BSC1 cells, taking advantage of the observation that more than 95% of the plasma–membrane clathrin-coated pits in these cells are rapidly forming, diffraction-limited structures [30]. The experiments were conducted in cells stably expressing fluorescently-tagged forms of clathrin light chain or σ2-adaptin, the small subunit of the endocytic clathrin adaptor AP-2. They were later extended to other cell types [22,34]. Regardless of cell type, the clathrin and AP-2 signals always colocalize.

In imaging studies of cells growing on a coverslip it is particularly important to distinguish the properties of clathrin-related processes at the free surface of a cell from those at the coverslip-attached surface. Clathrin-containing fluorescent structures detected at the free surface are, with rare exceptions, diffraction limited (below the ~250 nm optical resolution of the imaging setup). They show a characteristic steady protein accumulation, typically for a period of
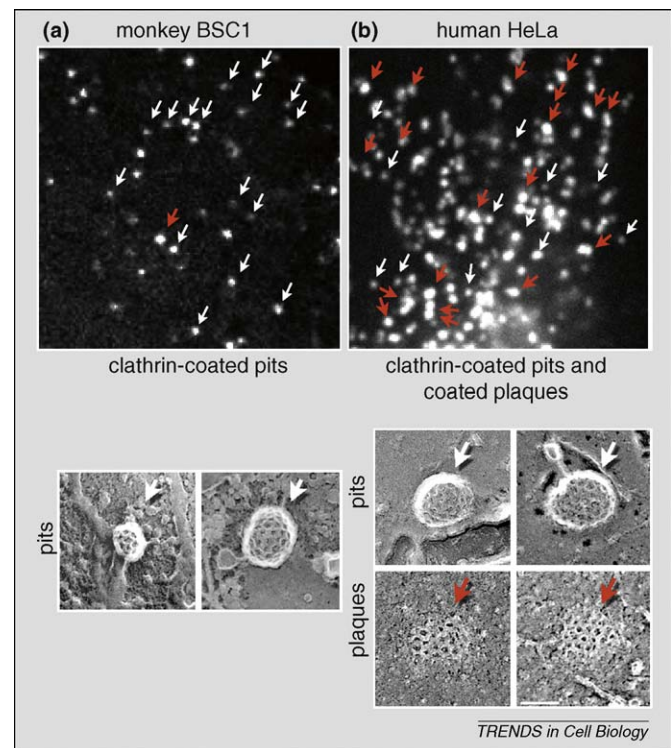

Figure 2. Different types of clathrin-coated structures detected on the attached surface of cells. The upper panels are single frames from time series recorded from: **(a)** a monkey BSC1 cell expressing σ2–EGFP of the adaptor AP-2; **(b)** a human HeLa cell expressing the Tomato–LCa light chain of clathrin. The live-cell images are from optical sections, acquired with a spinning disc confocal microscope, at the level at which plasma membrane adheres to the glass coverslip. The white and red arrows single out short- and long-lived fluorescent objects, whose dynamic behavior corresponds to coated pits and coated plaques, respectively. The bottom panels are electron micrographs obtained from the attached surfaces of 'unroofed' preparations of the corresponding cell type. Whereas BSC1 cells display only deeply curved clathrin-coated structures (pits), HeLa cells contain both deeply curved and relatively flat clathrin lattices (pits and plaques, respectively). The clathrin lattices in coated pits contain both hexagonal and pentagonal facets; the coated plaques contain mostly hexagonal facets.

40–70 s. They disappear suddenly at the end of the accumulation period because coat disassembly rapidly follows membrane budding. These events correspond to 'canonical'-coated pits, in which the sequential recruitment of clathrin and its adaptors results in a coat that assembles progressively into a curved lattice, deforming the membrane as it grows (Figure 1). In canonical-coated pits, adaptors selectively capture membrane-bound proteins destined for endocytosis; membrane pinching, mediated by dynamin, separates the fully formed coated vesicle from its parent membrane, and an ATP-dependent Hsc70 chaperone uncoats the released vesicle. A subset of these coated pits forms sequentially at preferred sites or 'hot spots' [29] (Figure 1).

Clathrin and AP-2 structures at the coverslip-attached surface have more diverse characteristics (Figure 2b). One set comprises diffraction-limited objects with the same dynamic properties as the canonical-coated pits observed on the top surface. Members of a second set are of variable size, sometimes slightly larger than diffraction limited, and they have relatively long lifetimes, usually greater than two minutes and sometimes longer than 15 minutes [21,25,28–30]. Just before dissolution, the full coat moves inwards towards the cell interior, bringing with it a portion of the underlying membrane, which then buds off in a
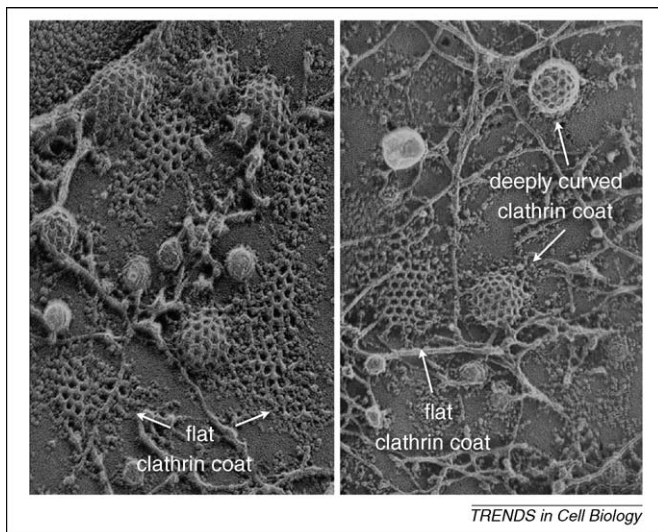
Figure 3. Morphology of clathrin-coated structures on the attached surface of cells. Electron micrograph obtained from an 'unroofed' preparation of human A4321 cells imaged by electron microscopy after quick-freeze deep-etching to show a range of different shapes of deeply curved and relatively flat clathrin structures on the adherent plasma membrane. (Reproduced, with permission, from [52]).

dynamin-dependent manner [26,34]. Classical images from electron microscopy (Figure 3) have shown extended clathrin lattices, approximately planar or moderately domed and with mostly hexagonal facets [52,53], called in one paper 'coated plaques' [54]. Recent work shows that the long-lived clathrin structures studied by live-cell imaging correspond, at least in many cases, to coated plaques (Figure 2) [34]. The relative abundance of coated plaques and canonical-coated pits depends strongly on cell type. For example, coated plaques are hard to observe in freshly plated BSC1 cells, whereas plaques lasting more than 15 minutes are dominant features on the adherent surface of HeLa cells.

'Non-terminal events' [25] is a phrase used to describe those cases in which a long-lived fluorescent clathrin structure remains in place, whereas a small drop in clathrin fluorescence in the overall object coincides with the formation and inward movement of a vesicular carrier marked (for example) by a fluorescent Tf receptor. The departing carrier contains only a small fraction of the total Tf receptor associated with the long-lived clathrin structure [26]. This type of event probably represents the formation and budding of a small clathrin-coated structure that is not spatially resolved from the coated plaque (i.e., separated from it by less than the 250 nm resolution limit of the light microscope). Indeed, electron micrographs of 'unroofed' cells often show deeply invaginated pits close to flat clathrin arrays (Figure 3).

Further experimental distinction between clathrin-coated pits and plaques comes from use of differential nanometry (DiNa), a high-z-precision ($\sim$10 nm) imaging technique that correlates the time dependence of fluorescence, recorded both by total internal reflection (TIR) and wide-field illumination, from two distinct components in an assembling structure [22]. DiNa, when applied to cells expressing fluorescently-tagged clathrin, AP-2 and epsin, has allowed the determination, with a temporal resolution of $\sim$1 s, of the relative displacement of AP-2

or epsin with respect to clathrin in endocytic structures forming on the attached membrane of mammalian cells [22,34].

DiNa measurements show that a canonical-coated pit grows continuously as an invaginating shell, which pinches off immediately upon completion. The entire process takes typically 30–60 seconds. AP-2 concentrates in the older part of the curved coat, away from the plasma membrane, whereas epsin resides primarily at the growing rim of the pit, closer to the plasma membrane. This polarized distribution of AP-2 corresponds to the asymmetric distribution of electron density in cryoEM tomographic reconstructions of coated vesicles isolated from the brain [55]. The polarized location of AP-2 with respect to clathrin in a budding coated pit explains why, under TIR conditions of illumination, the relative fluorescence of AP-2 decreases more rapidly than the corresponding fluorescence of clathrin, as the coated pit moves in the evanescent field away from the coverslip and towards the cell interior. Clathrin and AP-2 signals always disappear together when determined by spinning disc confocal or wide-field fluorescence microscopy. Thus, an earlier loss of the AP-2 signal determined by TIR does not imply a proposed alternative interpretation, in which AP-2 dissociates from the coat before disassembly of the clathrin lattice [23,56]. The well-established presence of both clathrin and AP-2 in coated vesicles isolated from tissues or cells also contradicts this alternative model.

By contrast, DiNa measurements show that a coated plaque grows initially at about the same rate as a coated pit, but without displacement from the cell surface. Its growth reaches a fluctuating plateau of fluorescence intensity, generally 2–3 times that of a typical pit, and the plaque remains in place for up to several minutes before moving uniformly inwards, a few seconds before membrane pinching. The fluctuation in the fluorescence signal might represent the partial addition and/or removal of clathrin and AP-2 from the coat, a behavior that is fully consistent with the partial fluorescence recovery after photobleaching (FRAP) of clathrin assemblies located at the bottom surface of HeLa cells [57]. In contrast to the relative displacement (with respect to clathrin) of AP-2 and epsin in coated pits, AP-2 and epsin have the same mean z-position as the bulk of the clathrin during the whole process of coated plaque formation [34].

Sharply curved pits and relatively flat, extended arrays have both been seen by electron microscopy (Figure 3), but there was no direct way to link the shape of the clathrin coats with their dynamic characteristics. The distinction between coated pits and coated plaques, derived from live-cell imaging, correlates with two kinds of lattices seen by standard transmission electron microscopy of thin sections or by freeze–etch electron microscopy on the inward-facing surface of adherent plasma membranes from 'unroofed' cells [53,54,58,59]. Recent work shows that the relative frequency of the two kinds of structures, as detected by electron microscopy, correlates well with their relative frequencies determined by live-cell imaging criteria. Specifically, BSC1 cells that display primarily short-lived clathrin events at the cell surface show only sharply curved pits when prepared for electron microscopy (Figure 2a, white arrows), whereas HeLa cells, which display both

short- and long-lived coated structures (Figure 2b, white and red arrows, respectively), show both sharply curved pits and extended clathrin lattices [34]. This correlation between clathrin lattice morphology and clathrin coat dynamics is fully consistent with the clathrin assembly model put forward more than 16 years ago [60]; this model also conforms to the structural constraints imposed by high-resolution cryoEM reconstructions of clathrin coats [17].

Many investigators assume that the flat clathrin sheets are an initial stage for coated pit formation and that curved 'domes' emerge by transforming hexagons into pentagons in the middle of an array. But the introduction of the proper number of pentagons (12) or combinations of heptagons–pentagons for curvature requires major molecular rearrangements. The intricate and extended association of legs from six different clathrin triskelions along any one edge makes the introduction of curvature (pentagons) into a flat (hexagonal) sheet exceptionally unlikely (see Figure 4 for an illustration of how clathrin triskelions are packed into the lattice and Figure 5 for an 'origami' exercise showing why such a rearrangement from hexagons to pentagons is implausible). The acquisition of a pentagon would require the stepwise removal of a 60° clathrin 'pie slice' (Figure 5), an operation that would have to be repeated 12 times. Not only are there no live-cell experimental data supporting such events, but also none of the necessary intermediates has ever been observed by electron microscopy. The internalization of a membrane coated by an extended, flat clathrin array, as occurs with coated plaques, involves an abrupt inwards movement into the cell of the entire coat [25,31,32,34,61]. Membrane invagination by a curved clathrin lattice, by contrast,

involves the continuous deformation linked to sequential addition of soluble triskelions [22,62].

Another distinction among different clathrin-based endocytic structures is their substantially different dependence on actin for the invagination and internalization of membrane. The assembly, budding and uncoating of canonical clathrin-coated pits in non-polarized cells such as BSC1 or HeLa are all insensitive to pharmacological interference with actin dynamics, at both the free and attached surfaces [51]. Canonical pits do not recruit actin-assembly regulators such as the Arp2/3 complex and cortactin [49]. By contrast, the formation and internalization of clathrin-coated plaques do involve the recruitment of these regulators but rather require normal actin dynamics [34].

Although coated pits and coated plaques seem to represent distinct assembly modes, there might also be 'hybrid' modes. VSV entry seems to be based on such a hybrid form of clathrin-mediated uptake. In that case, coat assembly proceeds normally in the absence of actin dynamics, as in canonical-coated pit formation, but budding does not occur until actin activity is restored [49]. Electron microscopy of endocytic VSV uptake suggests that the curved coat formation 'stalls' when the coated pit curves back against the shaft of the bullet-shaped virus particle [49]. These findings with VSV have parallels with the clathrin-dependent uptake of the bacterium *Listeria monocytogenes* [63,64]. Specifically, clathrin, dynamin, auxilin and actin are recruited during entry of both pathogens, and actin polymerization is crucial for their endocytosis but not for initial clathrin assembly. In addition, the localization of the actin machinery to sites of *L. monocytogenes* invasion requires the prior recruitment of clathrin and dynamin [64].

In summary, canonical-coated pits are invaginating structures, in which the assembly of a curved clathrin lattice, linked by adaptors and other proteins to the deformation of the underlying membrane, gives rise, by constriction and (dynamin-catalyzed) scission, to a coated vesicle (Figure 1b). After the early electron micrographs of yolk and LDL uptake [65,66], much subsequent work on a great variety of other cargo [67] and countless studies of membrane reuptake at presynaptic nerve endings [68] all illustrate this process. Extended clathrin lattices of low curvature (enriched in hexagonal arrays), now called clathrin-coated plaques, have also been observed for many years at the attached surface of cells [53,54,58,59], and their relationship to the canonical, curved assembly has now been resolved. The coated plaques internalize, but by a mechanism requiring actin remodeling, probably similar to the one proposed for clathrin-mediated membrane uptake in yeast cells [39]. In contrast to events in yeast cells, however, membrane scission in metazoan cells is catalyzed by dynamin.

Figure 4. Receptor sorting and clathrin-coated pit formation. Schematic representation of a clathrin lattice during the assembly of a deeply invaginated coated pit, obtained from the accompanying animation Movie 1. The shape and location of the triskelions are based on the map (resolution 0.8 nm) of a clathrin coat obtained by cryoEM [17]. The position of AP-2 within the coat is approximate. The shape of AP-2 is based on X-ray crystallographic data [10]. AP-2 adaptor complexes bind selectively to the plasma membrane by interacting both with PtdIns(4,5)P2 in the membrane bilayer and sorting motifs in the cytosolic tails of membrane-bound cargo receptors.

Abortive clathrin coats

Clathrin assemblies that fail to bud, referred to as 'abortive clathrin coats', can also be seen (Figure 1). First detected by global analysis of data obtained by spinning disc confocal microscopy [30], and later confirmed by global analysis of TIRF time series [69], abortive clathrin coats have typical lifetimes of less than 20 s. They contain less clathrin and
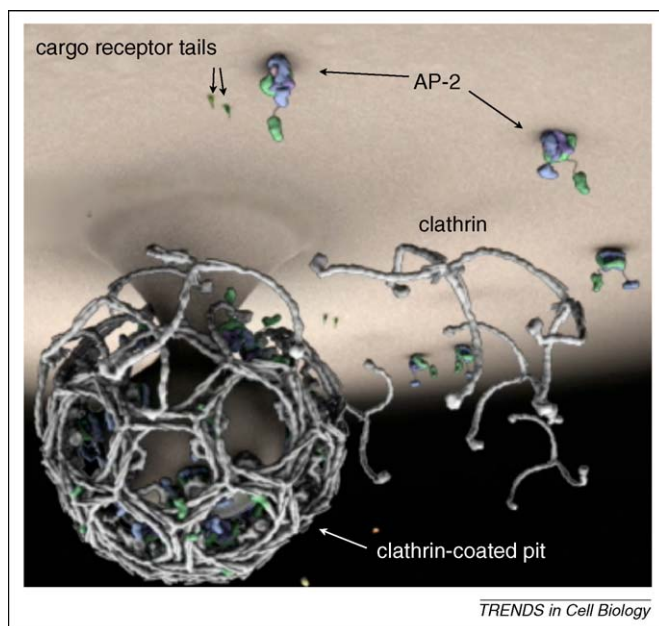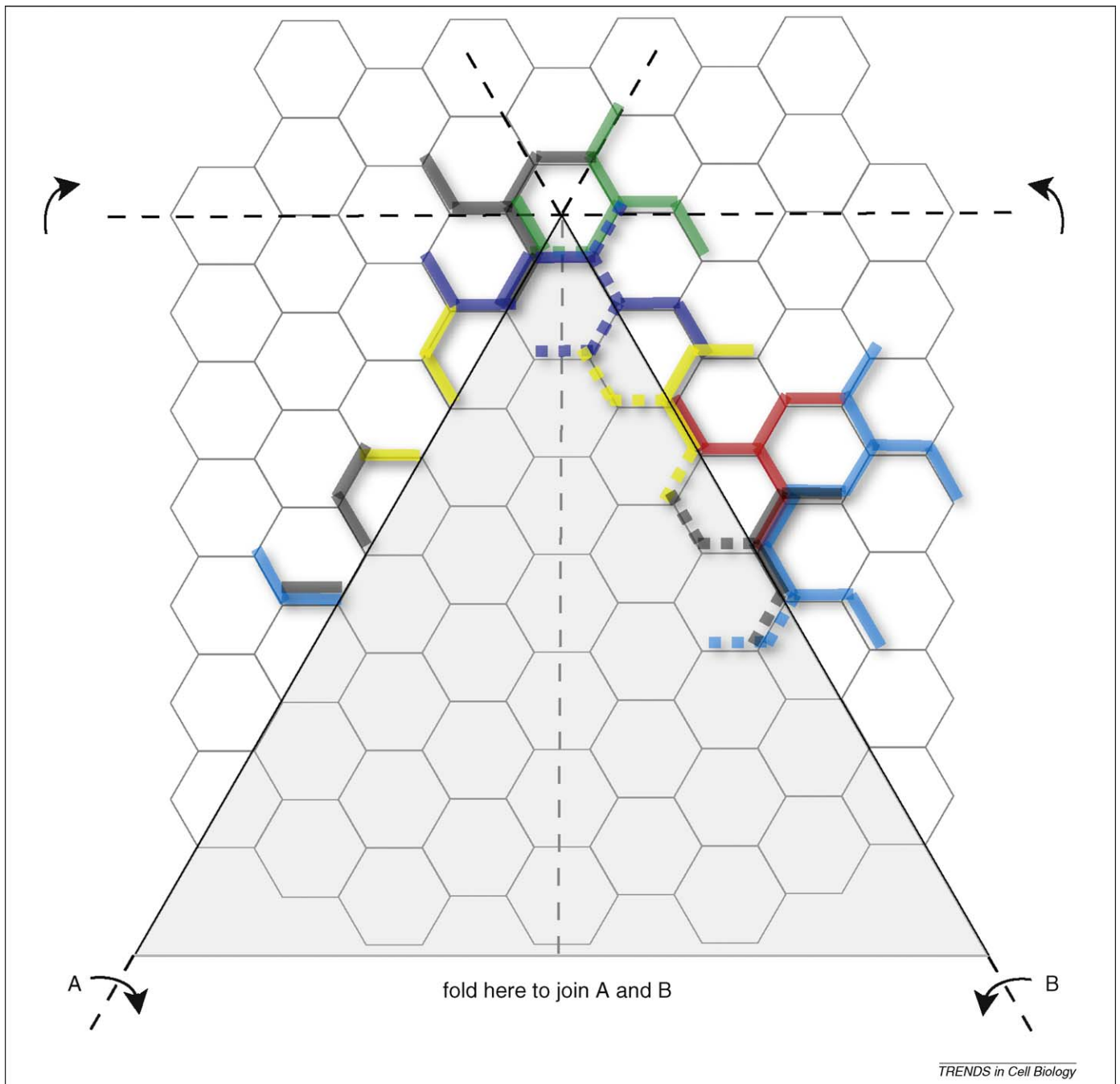
fold here to join A and B

TRENDS in Cell Biology

Figure 5. Rearrangements of clathrin triskelions in a flat hexagonal lattice that would be required to transform a single hexagon into a pentagon. This figure is adapted from [60]. If hexagonal sheets are indeed intermediates in the budding of coated pits, major rearrangements of this kind would be necessary. High-resolution structural data show that a triskelion is centered at every vertex, with each of its three legs spanning three consecutive edges [17,79]. To simplify the drawing, only a subset of color-coded triskelions is shown, depicting just their proximal and distal legs (those spanning the two edges closest to the vertex). Thick lines highlight a subset of triskelions that would need to refold into the new lattice; the color-coded stippled lines indicate the new positions adopted by the legs after the rearrangement. The reader is invited to print the diagram (adapted from [60]), cut out the gray triangular region and fold it along the lines indicated to generate a curved sheet. To make an approximately spherical clathrin lattice, 12 such rearrangements are required at precise locations within the lattice. This lattice contains 154 triskelions, and 72 would need to be removed (under the gray pie section) to transform a single hexagon into a pentagon. Eleven additional reductions (of different amounts, depending on the location of the new pentagons) are required to generate a completely enclosed structure. No such reductions have ever been detected during the formation of clathrin-coated structures. Clathrin is a relatively stiff protein (especially considering its contour length), with legs disposed at orientations relatively close to those adopted in the final coat [17]. Overall, coat formation can readily be understood by the sequential assembly of triskelions into a curved lattice. There is no need to postulate a flat, hexagonal intermediate, most of which would have to disassemble to generate curvature.

AP-2 than do canonical-coated pits at completion, and they are in some cases even more abundant than coated pits and plaques. It is currently believed that abortive clathrin coats represent nucleation and/or initiation events of coat components that start to assemble but then dissolve and fail to progress to invaginating structures because they do not associate with cargo. Evidence supporting this model comes from absence of LDLs, VSV or reovirus colocalization with abortive structures [30,49] and from the decrease in the number of abortive coats upon conditions of extreme overexpression of a Tf receptor [69], a membrane cargo actively internalized by clathrin-coated pits and plaques.

Role of actin

The relationship between clathrin and actin in endocytic membrane traffic seems to depend on the cell type and the kinds of clathrin structures involved. The relevant recruitment and switching mechanisms have not yet been fully worked out. Genetic and imaging data clearly show a strong link between clathrin and actin dynamics for endocytosis in yeast cells [31,32,39]. Live-cell imaging experiments that follow the recruitment of a large number of fluorescently-tagged proteins at locations marked by the transient appearance of clathrin demonstrate early transient accumulation of Las17, followed by the recruitment of clathrin and associated proteins such as Sla1, Pan1, End3, Sla2 or myosin V, and of actin and regulators of its assembly such as the Arp2/3 complex, Abp1, Cap1/2 and Sac6 [39]. These observations have been extended to metazoan cells, leading to the assumption that actin dynamics are essential both during early stages of clathrin coat formation and for budding. The assembly of endocytic clathrin coats at the free surface of non-polarized cells is actin-independent, however, just as for canonical-coated pits at the attached surface of the same cells. The formation of coated plaques at the attached surface does require actin dynamics [34], as does coat formation in some polarized cells [48,70]. Actin and clathrin dynamics are also linked during the internalization of VSV, even though the clathrin coat surrounding the virus is highly curved, and in the AP-2 adaptor-independent mode of clathrin array formation induced during phagocytic uptake of *L. monocytogenes* [64].

Hip1R is a regulator of actin dynamics that associates with the clathrin light chains cortactin and F-actin [71–74]. Like the loss of clathrin endocytic activity in yeast cells, interference with the clathrin light chains or Hip1R association with the clathrin light chains in (non-polarized) mammalian cells minimally affects the clathrin-mediated uptake of transferrin [74] and has no effect on the dynamics of canonical-coated pits, but does prevent the assembly of plaques [34]. These observations, that actin-dependent and actin-independent modes of clathrin assembly co-exist in the same cells, suggest that there are molecular signals that determine which mechanism of membrane deformation and budding will prevail. In VSV entry, there seems to be a switch, in which clathrin coat assembly proceeds normally in the absence of actin dynamics, but budding followed by coat disassembly does not [49]; in the same cells, canonical-coated pits form and pinch normally. Thus, the actin cytoskeleton has a variable role in clathrin-based endocytosis, and we expect that future analysis will reveal the mechanism(s) required to switch from one form to the other. Live-cell imaging designed to monitor single endocytic events has been instrumental in uncovering these relationships, which would otherwise have been confounded by the results of ensemble biochemical methodologies or the unconnected snapshots obtained from fixed cells.

Future directions

The availability of improved imaging hardware, including fast, reliable and sensitive digital cameras for data acquisition, automated motorized microscopes, correction of spherical aberration, strong light sources, *in situ* expression of chimeric fluorescent proteins, increased computational power, improved spatial resolution during live-cell imaging [22,75–77] and new analytical tools for unbiased detection of weak fluorescent events [78] should now allow investigators to gather information on early events in the initiation of coat formation, the regulation of assembly and disassembly, the relationships between the content of coat components and properties of different classes of clathrin-coated structures and whether the characteristics of endocytic clathrin coats in cells within tissues is the same as in cultured cells. Perhaps it will be possible to work out in detail how receptors are captured by adaptors, when SNAREs are recruited to a forming coat and the functions of the various 'flavors' of a clathrin coat. The availability of more robust data sets will also permit the generation of detailed kinetic and/or stochastic mathematical models that can then be used to test ideas and hypotheses of how clathrin coats form.

Unbiased methods are crucial for the proper analysis of a large population of relatively heterogeneous, spatio-temporal events, especially those that give relatively weak fluorescent signals. These approaches are particularly crucial when monitoring the kinds of single events detected by live-cell imaging. The first application of such an approach to clathrin-coated structures was based on the computational selection of events that satisfied the combined criteria of having a fluorescence intensity statistically higher than that of the surrounding background and a lifetime longer than 15 s [30]. This method allowed the detection of all clathrin-based endocytic events and the presence of abortive structures, but it was not sufficiently robust to track them. A more recent improved particle-tracking approach, also designed for unbiased detection, now allows both the detection and tracking of all clathrin-based endocytic processes [69,78].

Concluding remarks

High-resolution fluorescence imaging techniques have made it possible to classify distinct kinds of clathrin-containing endocytic objects: abortive, non-invaginating events; relatively shorter-lived, continuously invaginating, canonical-coated pits; and longer-lived, generally larger, non-curved structures (coated plaques). The coated plaques appear to be similar to the clathrin-containing, endocytic structures found in yeast cells. Different roles for actin dynamics have been identified for each of these modes of clathrin assembly, and there is a regulated interplay between clathrin assembly and actin dynamics. We now have an internally consistent mechanistic picture of how clathrin coats form, derived from the spatio-temporal characteristics of assembling clathrin objects obtained by live-cell imaging and the structural constraints imposed by high-resolution descriptions of the clathrin lattice.

References

1 McMahon, H.T. and Mills, I.G. (2004) COP and clathrin-coated vesicle budding: different pathways, common approaches. *Curr. Opin. Cell Biol.* 16, 379–391

2 Kirchhausen, T. (2000) Three ways to make a vesicle [Review]. *Nat. Rev. Mol. Cell Biol.* 1, 187–198

3 Robinson, M.S. (2004) Adaptable adaptors for coated vesicles. *Trends Cell Biol.* 14, 167–174

4 Bonifacino, J.S. and Traub, L.M. (2003) Signals for sorting of transmembrane proteins to endosomes and lysosomes. *Annu. Rev. Biochem.* 72, 395–447

5 Hirst, J. and Robinson, M.S. (1998) Clathrin and adaptors. *Biochem. Biophys. Acta* 1404, 173–193

6 Brodsky, F.M. *et al.* (2001) Biological basket weaving: formation and function of clathrin-coated vesicles. *Annu. Rev. Cell Dev. Biol.* 17, 517–568

7 Ungewickell, E.J. and Hinrichsen, L. (2007) Endocytosis: clathrin-mediated membrane budding. *Curr. Opin. Cell Biol.* 19, 417–425

8 Duncan, M.C. and Payne, G.S. (2005) Cell biology: protein choreography. *Nature* 438, 571–573

9 Traub, L.M. (2005) Common principles in clathrin-mediated sorting at the Golgi and the plasma membrane. *Biochim. Biophys. Acta* 1744, 415–437

10 Owen, D.J. *et al.* (2004) Adaptors for clathrin coats: structure and function. *Annu. Rev. Cell Dev. Biol.* 20, 153–191

11 Motley, A.M. *et al.* (2006) Functional analysis of AP-2 alpha and mu2 subunits. *Mol. Biol. Cell* 17, 5298–5308

12 Keyel, P.A. *et al.* (2006) A single common portal for clathrin-mediated endocytosis of distinct cargo governed by cargo-selective adaptors. *Mol. Biol. Cell* 17, 4300–4317

13 Gaidarov, I. and Keen, J.H. (2005) Membrane targeting of endocytic adaptors: cargo and lipid do it together. *Dev. Cell* 8, 801–802

14 Edeling, M.A. *et al.* (2006) Life of a clathrin coat: insights from clathrin and AP structures. *Nat. Rev. Mol. Cell Biol.* 7, 32–44

15 Brett, T.J. and Traub, L.M. (2006) Molecular structures of coat and coat-associated proteins: function follows form. *Curr. Opin. Cell Biol.* 18, 395–406

16 Miwako, I. and Schmid, S.L. (2006) A cell-free biochemical complementation assay reveals complex and redundant cytosolic requirements for LRP endocytosis. *Exp. Cell Res.* 312, 1335–1344

17 Fotin, A. *et al.* (2004) Molecular model for a complete clathrin lattice from electron cryomicroscopy. *Nature* 432, 573–579

18 Murray, J.M. *et al.* (2007) Evaluating performance in three-dimensional fluorescence microscopy. *J. Microsc.* 228, 390–405

19 Waters, J.C. (2009) Accuracy and precision in quantitative fluorescence microscopy. *J. Cell Biol.* 185, 1135–1148

20 Zoncu, R. *et al.* (2007) Loss of endocytic clathrin-coated pits upon acute depletion of phosphatidylinositol 4,5-bisphosphate. *Proc. Natl. Acad. Sci. U. S. A.* 104, 3793–3798

21 Yarar, D. *et al.* (2005) A dynamic actin cytoskeleton functions at multiple stages of clathrin-mediated endocytosis. *Mol. Biol. Cell* 16, 964–975

22 Saffarian, S. and Kirchhausen, T. (2008) Differential evanescence nanometry: live-cell fluorescence measurements with 10 nm axial resolution on the plasma membrane. *Biophys. J.* 94, 2333–2342

23 Rappoport, J.Z. *et al.* (2005) Analysis of the AP-2 adaptor complex and cargo during clathrin-mediated endocytosis. *Traffic* 6, 539–547

24 Rappoport, J.Z. *et al.* (2006) Dynamics of clathrin and adaptor proteins during endocytosis. *Am. J. Physiol. Cell Physiol.* 291, C1072–1081

25 Merrifield, C.J. *et al.* (2002) Imaging actin and dynamin recruitment during invagination of single clathrin-coated pits. *Nat. Cell Biol.* 4, 691–698

26 Merrifield, C.J. *et al.* (2005) Coupling between clathrin-coated pit invagination, cortactin recruitment and membrane scission observed in live cells. *Cell* 121, 593–606

27 Le Clainche, C. *et al.* (2007) A Hip1R-cortactin complex negatively regulates actin assembly associated with endocytosis. *EMBO J.* 26, 1199–1210

28 Keyel, P.A. *et al.* (2004) Endocytic adaptor molecules reveal an endosomal population of clathrin by total internal reflection fluorescence microscopy. *J. Biol. Chem.* 279, 13190–13204

29 Gaidarov, I. *et al.* (1999) Spatial control of coated pit dynamics in living cells. *Nat. Cell Biol.* 1, 1–7

30 Ehrlich, M. *et al.* (2004) Endocytosis by random initiation and stabilization of clathrin-coated pits. *Cell* 118, 591–605

31 Kaksonen, M. *et al.* (2005) A modular design for the clathrin- and actin-mediated endocytosis machinery. *Cell* 123, 305–320

32 Newpher, T.M. *et al.* (2005) *In vivo* dynamics of clathrin and its adaptor-dependent recruitment to the actin-based endocytic machinery in yeast. *Dev. Cell* 9, 87–98

33 Mettlen, M. *et al.* (2009) Endocytic accessory proteins are functionally distinguished by their differential effects on the maturation of clathrin-coated pits. *Mol. Biol. Cell* 20, 3251–3260

34 Saffarian, S. *et al.* (2009) Distinct dynamics of endocytic clathrin-coated pits and coated plaques. *PLoS Biol.* 7, e1000191

35 Hofmann, M. *et al.* (2005) Breaking the diffraction barrier in fluorescence microscopy at low light intensities by using reversibly photoswitchable proteins. *Proc. Natl. Acad. Sci. U. S. A.* 102, 17565–17569

36 Huang, B. *et al.* (2008) Whole-cell 3D STORM reveals interactions between cellular structures with nanometer-scale resolution. *Nat. Methods* 5, 1047–1052

37 Macia, E. *et al.* (2006) Dynasore, a cell-permeable inhibitor of dynamin. *Dev. Cell* 10, 839–850

38 Rappoport, J.Z. *et al.* (2008) Dynamics of dynamin during clathrin mediated endocytosis in PC12 cells. *PLoS ONE* 3, e2416

39 Kaksonen, M. *et al.* (2006) Harnessing actin dynamics for clathrin-mediated endocytosis. *Nat. Rev. Mol. Cell Biol.* 7, 404–414

40 Engqvist-Goldstein, A.E.Y. and Drubin, D.G. (2003) Actin assembly and endocytosis: from yeast to mammals. *Annu. Rev. Cell Dev. Biol.* 19, 287–332

41 Merrifield, C.J. *et al.* (2004) Neural Wiskott Aldrich Syndrome Protein (N-Wasp) and the Arp2/3 complex are recruited to sites of clathrin-mediated endocytosis in cultured fibroblasts. *Eur. J. Cell Biol.* 83, 13–18

42 Benesch, S. *et al.* (2005) N-Wasp deficiency impairs EGF internalization and actin assembly at clathrin-coated pits. *J. Cell Sci.* 118, 3103–3115

43 Zhu, J. *et al.* (2005) Regulation of cortactin/dynamin interaction by actin polymerization during the fission of clathrin-coated pits. *J. Cell Sci.* 118, 807–817

44 Lamaze, C. *et al.* (1997) The actin cytoskeleton is required for receptor-mediated endocytosis in mammalian cells. *J. Biol. Chem.* 272, 20332–20335

45 Bourne, J. *et al.* (2006) Actin polymerization regulates clathrin coat maturation during early stages of synaptic vesicle recycling at lamprey synapses. *J. Comp. Neurol.* 497, 600–609

46 Shupliakov, O. *et al.* (2002) Impaired recycling of synaptic vesicles after acute perturbation of the presynaptic actin cytoskeleton. *Proc. Natl. Acad. Sci. U. S. A.* 99, 14476–14481

47 Sun, X. and Whittaker, G.R. (2007) Role of the actin cytoskeleton during influenza virus internalization into polarized epithelial cells. *Cell Microbiol.* 9, 1672–1682

48 Gottlieb, T.A. *et al.* (1993) Actin microfilaments play a critical role in endocytosis at the apical but not the basolateral surface of polarized epithelial cells. *J. Cell Biol.* 120, 695–710

49 Cureton, D.K. *et al.* (2009) Vesicular stomatitis virus enters cells through vesicles incompletely coated with clathrin that depend upon actin for internalization. *PLoS Pathog.* 5, e1000394

50 Sankaranarayanan, S. *et al.* (2003) Actin has a molecular scaffolding, not propulsive, role in presynaptic function. *Nat. Neurosci.* 6, 127–135

51 Boucrot, E. *et al.* (2006) Role of lipids and actin in the formation of clathrin-coated pits. *Exp. Cell Res.* 312, 4036–4048

52 Fujimoto, L.M. *et al.* (2000) Actin assembly plays a variable, but not obligatory role in receptor-mediated endocytosis. *Traffic* 1, 161–171

53 Heuser, J. (1980) Three-dimensional visualization of coated vesicle formation in fibroblasts. *J. Cell Biol.* 84, 560–583

54 Maupin, P. and Pollard, T. (1983) Improved preservation and staining of HeLa cell actin filaments, clathrin-coated membranes, and other cytoplasmic structures by tannic acid-glutaraldehyde-saponin fixation. *J. Cell Biol.* 96, 51–62

55 Cheng, Y. *et al.* (2007) Cryo-electron tomography of clathrin-coated vesicles: structural implications for coat assembly. *J. Mol. Biol.* 365, 892–899

56 Rappoport, J.Z. *et al.* (2003) The AP-2 complex is excluded from the dynamic population of plasma membrane-associated clathrin. *J. Biol. Chem.* 278, 47357–47360

57 Wu, X. *et al.* (2001) Clathrin exchange during clathrin-mediated endocytosis. *J. Cell Biol.* 155, 291–300

58 Aggeler, J. *et al.* (1983) High-resolution three-dimensional views of membrane-associated clathrin and cytoskeleton in critical point-dried macrophages. *J. Cell Biol.* 97, 1452–1458

59 Aggeler, J. and Werb, Z. (1982) Initial events during phagocytosis by macrophages viewed from outside and inside the cell: membrane–particle interactions and clathrin. *J. Cell Biol.* 94, 613–623

60 Kirchhausen, T. (1993) Coated pits and coated vesicles – sorting it all out. *Curr. Opin. Struct. Biol.* 3, 182–188

61 Idrissi, F.Z. *et al.* (2008) Distinct acto/myosin-I structures associate with endocytic profiles at the plasma membrane. *J. Cell Biol* 180, 1219–1232

62 Perera, R.M. *et al.* (2006) Two synaptojanin 1 isoforms are recruited to clathrin-coated pits at different stages. *Proc. Natl. Acad. Sci. U. S. A.* 103, 19332–19337

63 Veiga, E. and Cossart, P. (2006) The role of clathrin-dependent endocytosis in bacterial internalization. *Trends Cell Biol.* 16, 499–504

64 Veiga, E. *et al.* (2007) Invasive and adherent bacterial pathogens co-opt host clathrin for infection. *Cell Host & Microbe* 2, 340–351

65 Anderson, R.G. *et al.* (1977) Role of the coated endocytic vesicle in the uptake of receptor-bound low density lipoprotein in human fibroblasts. *Cell* 10, 351–364

66 Roth, T.F. and Porter, K.R. (1964) Yolk protein uptake in the oocyte of the mosquito *Aedes aegypti*. L. *Cell Biol.* 20, 313–331

67 Hanover, J.A. *et al.* (1985) Transit of receptors for epidermal growth factor and transferrin through clathrin-coated pits. Analysis of the kinetics of receptor entry. *J. Biol. Chem.* 260, 15938–15945

68 Newton, A.J. *et al.* (2006) Inhibition of dynamin completely blocks compensatory synaptic vesicle endocytosis. *Proc. Natl. Acad. Sci. U. S. A.* 103, 17955–17960

69 Loerke, D. *et al.* (2009) Cargo and dynamin regulate clathrin-coated pit maturation. *PLoS Biol.* 7, e57

70 Buss, F. *et al.* (2001) Myosin VI isoform localized to clathrin-coated vesicles with a role in clathrin-mediated endocytosis. *EMBO J.* 20, 3676–3684

71 Engqvist-Goldstein, A.E.Y. *et al.* (2001) The actin-binding protein Hip1R associates with clathrin during early stages of endocytosis and promotes clathrin assembly *in vitro*. *J. Cell Biol.* 154, 1209–1223

72 Chen, C-Y. and Brodsky, F.M. (2005) Huntingtin-interacting protein 1 (Hip1) and Hip1-related protein (Hip1R) bind the conserved sequence of clathrin light chains and thereby influence clathrin assembly *in vitro* and actin distribution *in vivo*. *J. Biol. Chem.* 280, 6109–6117

73 Legendre-Guillemin, V. *et al.* (2005) Huntingtin interacting protein 1 (HIP1) regulates clathrin assembly through direct binding to the regulatory region of the clathrin light chain. *J. Biol. Chem.* 280, 6101–6108

74 Poupon, V. *et al.* (2008) Clathrin light chains function in mannose phosphate receptor trafficking via regulation of actin assembly. *Proc. Natl. Acad. Sci. U. S. A.* 105, 168–173

75 Hein, B. *et al.* (2008) Stimulated emission depletion (STED) nanoscopy of a fluorescent protein-labeled organelle inside a living cell. *Proc. Natl. Acad. Sc.i U. S. A.* 105, 14271–14276

76 Eggeling, C. *et al.* (2009) Direct observation of the nanoscale dynamics of membrane lipids in a living cell. *Nature* 457, 1159–1162

77 Manley, S. *et al.* (2008) High-density mapping of single-molecule trajectories with photoactivated localization microscopy. *Nat. Methods* 5, 155–157

78 Jaqaman, K. *et al.* (2008) Robust single-particle tracking in live-cell time-lapse sequences. *Nat. Methods* 5, 695–702

79 Musacchio, A. *et al.* (1999) Functional organization of clathrin in coats: combining electron cryomicroscopy and X-ray crystallography. *Mol. Cell* 3, 761–770